REPORT

Loss of Axin1 in limb mesenchymal cells leads to multiple synostoses syndrome-like phenotype in mice

Dan Yi,[1,2] Rong Xie,[3] Daofu Zeng,[1,2] Jun Xiao,[4] Guozhi Xiao,[5] Hongting Jin,[6,*] Liping Tong,[1,*] and Di Chen[1,2,*]

*Correspondence: di.chen@siat.ac.cn (D.C.); lp.tong@siat.ac.cn (L.T.); hongtingjin@163.com (H.J.)

Received: July 20, 2023; Accepted: January 30, 2024; Published Online: February 22, 2024; https://doi.org/10.59717/j.xinn-med.2024.100053

GRAPHICAL ABSTRACT

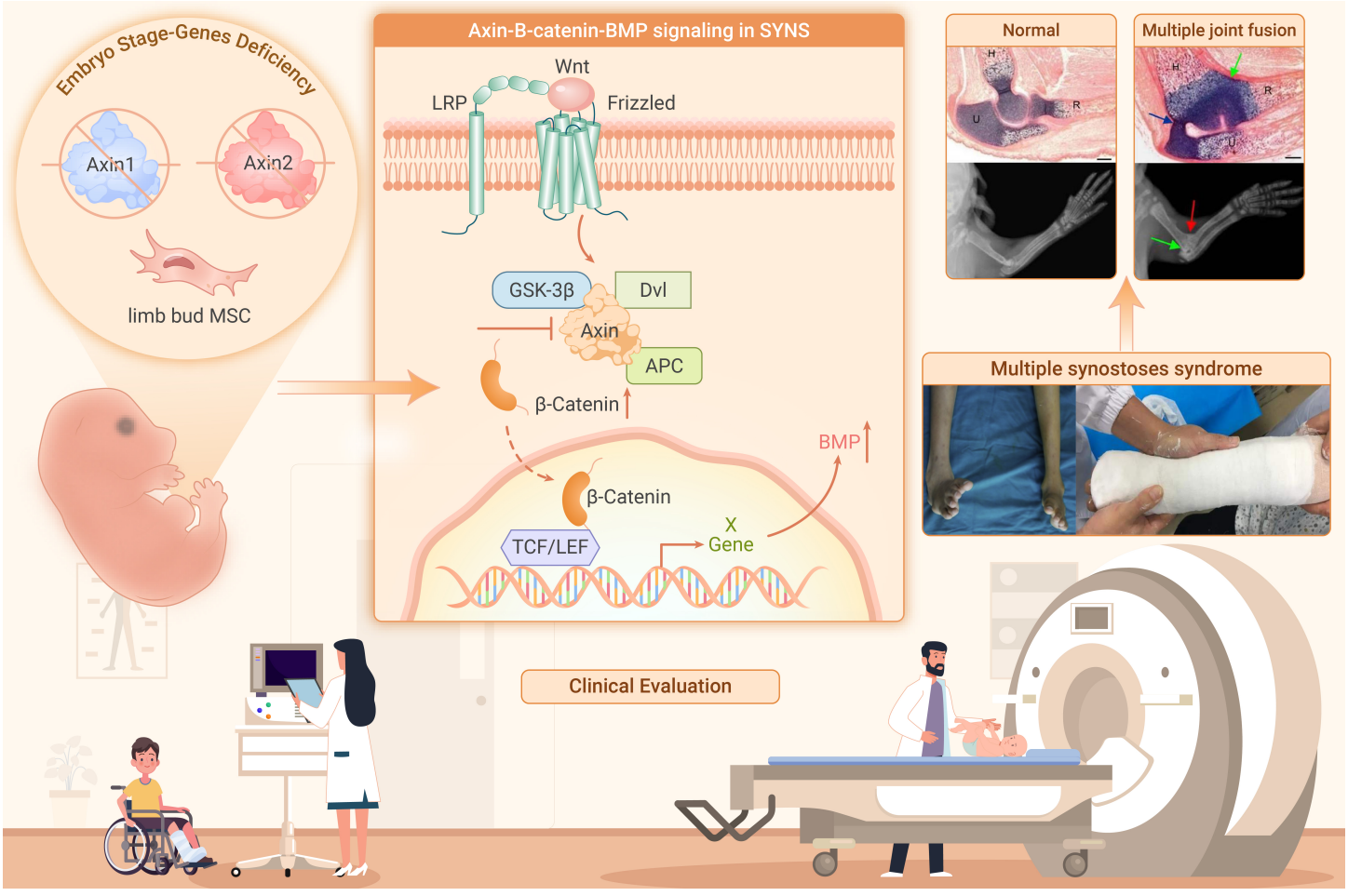

PUBLIC SUMMARY

- Loss-of-Axin1 or Axin1/Axin2 in limb MSCs in mice results in a phenotype resembling SYNS.
- Loss-of-Axins in limb MSCs in mice lead to the activation of β-catenin-BMP signaling in the cKO mice model.
- The SYNS phenotype in *Axin1* cKO mice could be partially reversed by β-catenin or BMP signaling inhibitor.
- The genetic mouse model with SYNS-like phenotype could serve as important tools for SYNS disease.

REPORT

www.the-innovation.org/medicine

Loss of Axin1 in limb mesenchymal cells leads to multiple synostoses syndrome-like phenotype in mice

Dan Yi,[1,2] Rong Xie,[3] Daofu Zeng,[1,2] Jun Xiao,[4] Guozhi Xiao,[5] Hongting Jin,[6,*] Liping Tong,[1,*] and Di Chen[1,2,*]

[1]Research Center for Computer-aided Drug Discovery, Shenzhen Institute of Advanced Technology, Chinese Academy of Sciences, Shenzhen 518005, China

[2]Faculty of Pharmaceutical Sciences, Shenzhen Institute of Advanced Technology, Shenzhen 518055, China

[3]Department of Orthopedic Surgery, Rush University Medical Center, Chicago 60612, USA

[4]Department of Orthopaedics, NanFang Hospital, Southern Medical University, Guangzhou 510515, China

[5]School of Medicine, Southern University of Science and Technology, Shenzhen 518055, China

[6]The First College of Clinical Medicine, Zhejiang Chinese Medical University and Institute of Orthopaedics and Traumatology of Zhejiang Province, Hangzhou 310053, China

*Correspondence: di.chen@siat.ac.cn (D.C.); lp.tong@siat.ac.cn (L.T.); hongtingjin@163.com (H.J.)

Received: July 20, 2023; Accepted: January 30, 2024; Published Online: February 22, 2024; https://doi.org/10.59717/j.xinn-med.2024.100053

Citation: Yi D., Xie R., Zeng D., et al., (2024). Loss of Axin1 in limb mesenchymal cells leads to multiple synostoses syndrome-like phenotype in mice. The Innovation Medicine **2(1)**: 100053.

Multiple synostoses syndrome (SYNS) is a disease characterized by the fusion of multiple joints. Unfortunately, the underlying and critical signaling pathways of this disorder remain poorly understood. Given the pivotal role of Wnt/β-catenin signaling in skeletal development and the key regulatory effect of Axin1 and Axin2 in the β-catenin pathway, limb mesenchymal stem cell (MSC) specific *Axin1* conditional KO (cKO) mice and *Axin1*/*Axin2* double KO (dKO) mice were generated to explore their involvement in joint formation. Abnormalities, such as developmental defects in joints and fusions in multiple joint tissues were observed in both *Axin1* cKO and *Axin1*/*Axin2* dKO mice, which resemble to the characteristics of human SYNS disease including synostoses of carpal and tarsal bones, as well as ankylosis of elbow joint and knee joint. Administration of β-catenin or BMP inhibitor significantly reversed the joint fusion phenotype in *Axin1* cKO mice. Our findings suggest that Axin1 plays a key role in joint formation by inhibiting β-catenin-BMP signaling and could potentially serve as a therapeutic target for SYNS.

INTRODUCTION

Multiple synostoses syndrome (SYNS) encompasses a spectrum of related genetic skeletal disorders characterized by varying degrees of multiple joint fusions, including symphalangism, carpal and tarsal synostoses.[1,2] Symphalangism can involve both proximal and distal phalanges of a finger or toe, with the fusion of proximal phalanges being the most frequent defect in SYNS. Additional features such as synostoses of multiple bones, phalanges deficiency, metacarpals shortening, and maxillofacial malformation (including nasal alar hypoplasia and vermilion margin on upper lip) have also been observed.[2] Furthermore, some individuals with SYNS may experience conductive deafness, often attributed to the fusion of hearing bones in the middle ear.[3] These abnormalities may represent independently or in association with each other.

Genetic testing conducted on unrelated families have revealed that SYNS is inherited as an autosomal dominant trait.[4,5] Currently, mutations in several genes encoding proteins important in BMP and FGF signaling have been identified in individuals with SYNS, including NOG, GDF5, GDF6, and FGF9 which are considered pathogenic genes of SYNS.[5-12] Mutations in these genes lead to significant alterations in BMP, TGF-β, and FGF signaling pathways. The majority of SYNS causes are believed to be associated with disorders of cartilage and bone development. While the canonical Wnt/β-catenin signaling pathway is known to regulate bone and cartilage development and closely interacts with BMP, TGF-β and FGF signaling pathways,[13-15] the contribution of Wnt/β-catenin signaling in SYNS has not been investigated until now.

The canonical Wnt signaling cascades are indispensable in embryonic development and regulate various biological processes in the body, including organogenesis, postnatal tissue growth, homeostasis maintenance, and disease development.[16-20] Genetic evidence suggests the critical role of Wnt signaling in controlling bone development, including craniofacial and limb development, as well as joint formation.[21,22] A key regulatory mechanism underlying this pathway is achieved through the dynamic degradation of β-catenin by the cytoplasmic 'destruction complex'. Axin1 and Axin2 serve as central and rate-limiting scaffolding proteins in this destruction complex, indicating that both Axin1 and Axin2 are inverse regulators of the classical β-catenin signaling pathway. Studies have reported that *Axin2*$^{-/-}$ mice manifest craniosynostosis during cranial bone morphogenesis,[13] which is a typical clinical feature of SYNS. Our prior study demonstrated that the deletion of *Axin1* in *Prrx1*-expressing limb mesenchymal cells results in a phenotype resembling human fibular hemimelia disease,[23] suggesting the significant role of Axin1 in joint development. In addition, Axin inhibitors have been previously developed as important tools to antagonizing Wnt signaling.[24] Based on these findings, we hypothesize that Axin1 may play a pivotal role in joint development and prevent joint fusion. However, due to the early embryonic lethality associated with *Axin1* mutation, the *in vivo* role of Axin1 in synostoses has yet to be fully elucidated.[25]

In this study, a conditional knockout (cKO) approach was conducted to investigate the roles of *Axin1* and *Axin2* in SYNS. Results revealed that the deletion of *Axin1* and *Axin2* in limb mesenchymal cells (MSCs) results in SYNS-like phenotype, characterized by carpal and tarsal synostoses, as well as fusions of the elbow joint and knee joint. These findings highlight the pivotal role of Axin1 and Axin2 in regulating skeletal development and joint formation through controlling β-catenin-BMP signaling in limb tissues. The current work not only elucidates the pathogenesis of SYNS, but also presents novel animal models that can be further utilized to explore the pathological mechanisms and treatment strategies for SYNS.

MATERIALS AND METHODS

Mice

Axin1-flox mice and *Prrx1-Cre* transgenic mice were intercrossed to generate conditional *Axin1* mutant animal model, named as *Axin1*^{Prrx1} cKO mice.[26] *Axin1*$^{flox/flox}$ mice were used in previous studies.[26] All genders of *Axin1*$^{flox/flox}$ mice are viable and fertile, with no identifiable phenotype. *Ctnnb1* (*β-catenin*$^{flox/flox}$) mice were constructed by floxing the exons 2-6 of the β-catenin gene,[27] and were kindly given by Jackson Laboratory. Axin1/Axin2 dKO mice were generated by breeding the *Axin1*^{Prrx1} cKO mice with *Axin2*$^{-/-}$ mice. All mice were kept in SPF laboratory under standard conditions. Animal experiments were approved by the Animal Investigation Ethics Committee of Rush University and SIAT.

In the rescue experiments, half Cre-positive mice (*Axin1*$^{flox/flox}$;*Prrx1-Cre* mice) and half Cre-negative mice (*Axin*$^{flox/flox}$) were bred together to generate 50% *Axin1* cKO mice and 50% Cre-negative control mice. The mice (pregnant mothers) were randomly divided and given a single dose of β-catenin inhibitor iCRT14 (Tocris, Minneapolis, MN, USA, 2.5 mg/kg body weight), Wnt secretion inhibitor LGK974 (Selleck, Houston, TX, USA, 2.5 mg/kg body weight), BMP inhibitor dorsomorphin (Tocris, Minneapolis, MN, USA, 2.5 mg/kg body weight), Axin2 agonists IWR-1-endo (Selleckchem, Houston, TX, USA, 2.5 mg/kg body weight) or TGF-β inhibitor SB-505124 (Adooq Bioscience, Nanjing, China, 2.5 mg/kg body weight), i.p. injection, to the pregnant mice at E9.5 stage, respectively.

Alizerin red/Alcian blue staining

Whole skeletons were fixed in 95% ethanol for 2 days. The skeletons were then immersed in acetone for an additional day to remove the residual fat. The skeletons were stained with 0.015% alcian blue and 0.005% alizarin red

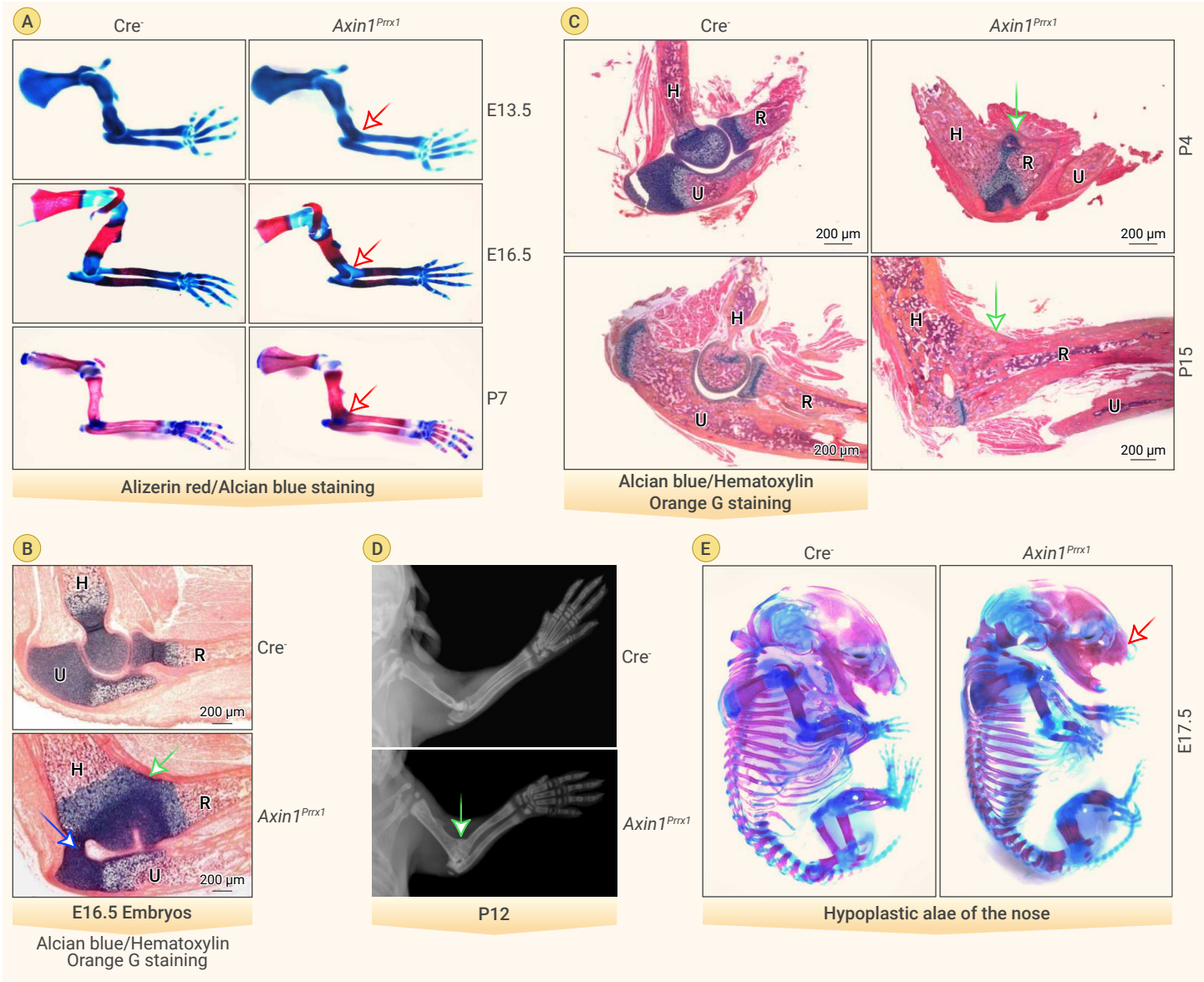

Figure 1. Deletion of *Axin1* in limb mesenchymal progenitor cells resulted in defects in the upper joint (A) The fusion of elbow joint was observed in *Axin1* cKO embryos and postnatal mice. Alizerin red/Alcian blue staining was performed in forelimbs of E13.5 and E16.5 embryos, and postnatal day 7 (P7) mice. Red arrows: joint fusions observed in E13.5, E16.5 and P7 *Axin1* cKO embryos and mice. (B&C) Alcian blue/Hematoxylin & Orange G (AB/HOG) staining of histological sections of E16.5 embryos (B) and postnatal P4 and P15 mice (C) showed fusion of humerus (H) and radius (R) (green arrows) and fusion of humerus (H) and ulna (U) (blue arrow). (D) X-ray radiographic analysis also showed fusion of elbow joint (green arrow) in postnatal *Axin1* cKO mice (P12). (E) Alizerin red/Alcian blue staining of E17.5 of *Axin1* cKO embryos showed hypoplastic alae of the nose (red arrow).

for 3 days.

The skeletons were then washed several times with eluent composed of PBS and ethanol, and further cleared by 1% potassium hydroxide. The stained skeletons were stored in 100% glycerol.[28]

Histology

Histology analysis was employed to evaluate the multiple synostoses. In brief, the collected samples were fixed with 10% neutral formalin (VWR, 16004-128), decalcified by formic acid and rinsed with floating water for 12-24 hours. After that, the samples were embedded in paraffin and sliced at the thickness of 4 μm. The tissue sections were then stained with Alcian blue/hematoxylin and eosin (ABH) and Orange G following standard procedure. The stained samples were imaged and the captured using the Olympus BX43 microscope with CellSens Imaging Software (Olympus).

X-ray radiographic analysis

After euthanasia, the mouse skeletons were radiographed by Faxitron Cabinet X-ray system (Faxitron X-ray, Wheeling, IL).

Micro-CT analysis

The fixed bone and knee joints were scanned by μCT-35 cone-beam scanner (Scanco Medical) with a 55 kVp source and a 145 μAmp current at a resolution of 10 μm. Then samples 100 slices extending proximally were applied for scanning starting from where the tibia condyle had been found fully merged. The reconstructed 3-dimensional images for each sample were assessed at the same thresholds.

Immunohistochemical (IHC) analysis

Knee joint sections were immersed in Antigen Unmasking Solution at 95°C for 10 min and then treated with 3% H_2O_2, 0.5% Triton X-100 and Avidin/Biotin Blocking Kit to avoid the non-specific binding and to improve binding efficiency of antibody. After blocking with 10% goat serum for 1h, the tissue sections were incubated with primary antibody (BMP2 antibody, ab284387) and biotinylated goat anti-rabbit antibody (BE0101, Easybio, China), respectively. Samples were finally treated with VECTASTAIN Elite ABC Kit (Vector Laboratories) and IHC signals were labeled by ImmPACT DAB peroxidase substrate (Vector Laboratories).

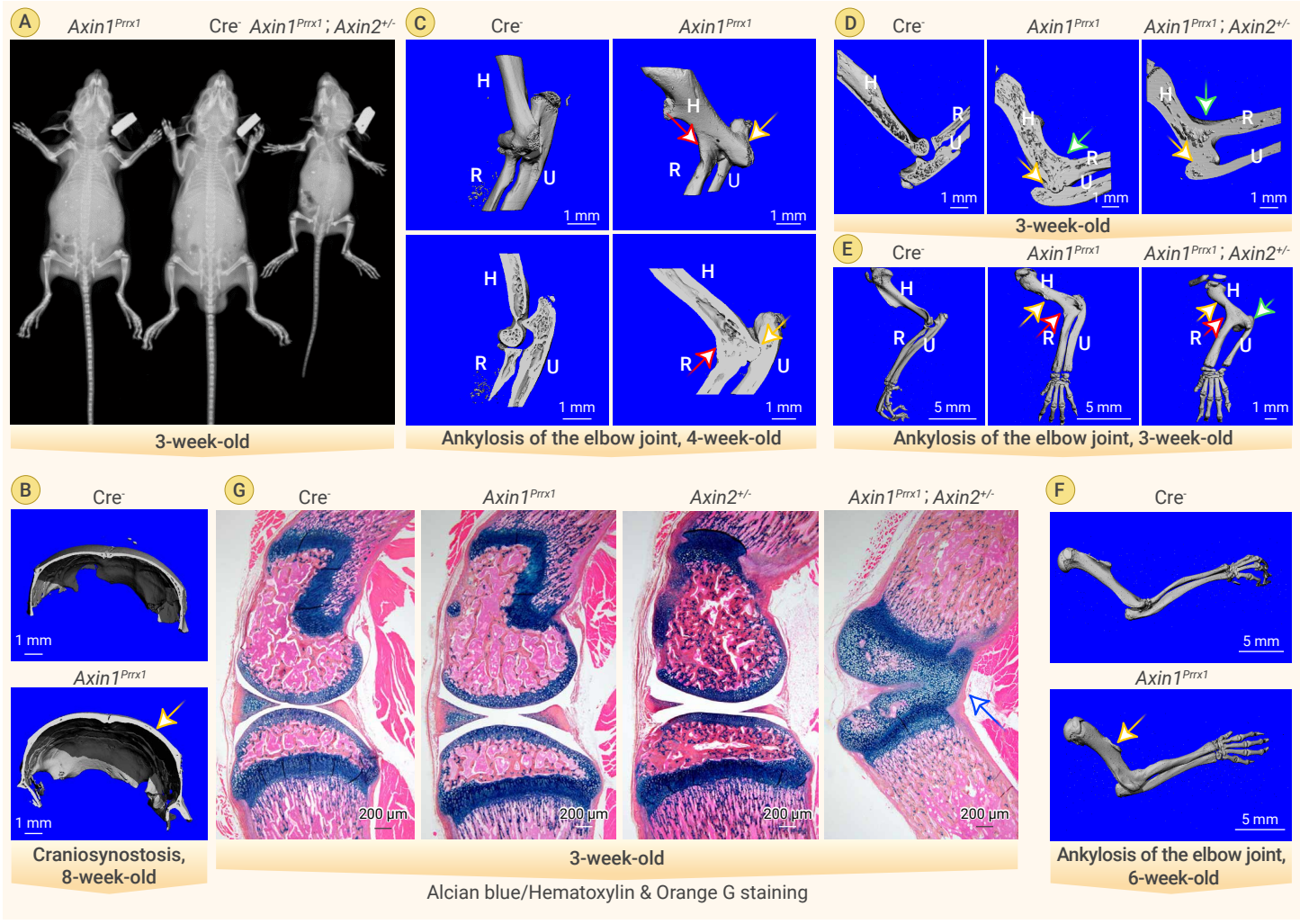

Figure 2. Multiple synostoses-like phenotype in upper limb of *Axin1* cKO mice and *Axin1*/*Axin2* dKO mice (A) Radiographic analysis (x-ray) presented an obviously smaller body size of 3-week-old (3-wk-old) *Axin1*/*Axin2* dKO mice than Cre$^-$ and *Axin1* cKO mice. (B) μCT analysis showed three-dimensional volumetric reconstructions of skulls showing bone mass was increased in *Axin1* cKO mice. (C) μCT analysis showed 3D reconstructed images of elbow joints of 4-week-old mice. Red arrows indicated fusion of humerus (H) and radius (R). Yellow arrows indicated fusion of humerus (H) and ulna (U). (D) μCT analysis (2D images) also demonstrated elbow joint fusion in *Axin1* cKO mice and remarkably more severe joint fusion in 3-week-old *Axin1*/*Axin2* dKO mice. (E&F) Micro-CT results indicated that 3- and 6-week-old *Axin1* cKO mice or *Axin1*/*Axin2* dKO mice had elbow joint fusion (yellow arrows) and loss of deltoid tuberosity structure (red arrows). The *Axin1*/*Axin2* dKO mice had a more severe phenotype than *Axin1* KO mice. (G) Alcian blue histology staining showed knee joint fusion in *Axin1*/*Axin2* dKO mice.

Cell culture and qPCR

C3H10T1/2 mesenchymal progenitor cells were cultured in α-MEM supplemented with 10% fetal bovine serum (FBS) and 1% v/v penicillin/streptomycin. Cells were grown at 37°C and 5% CO_2 in a humidified incubator. Cells were treated with various siRNAs (RIBOBIO, Guangzhou, China; Table S1) for 48 hours. Total RNA was extracted by Trizol (Invitrogen Life Technologies, 15596026). 1 μg total RNA was loaded to synthesize complementary DNA (cDNA) withHiScript® III All-in-one RT SuperMix Perfect for qPCR (Vazyme, R333). Next, real-time PCR amplification was completed with specific primers (Table S2) of genes and AceQ® Universal SYBR qPCR Master Mix (Vazyme, Q511). The names and sequences of certain primers are listed in Table S2. Data were analyzed by collecting chondrocytes from 3 independent mice per group (n = 3).

Western Blot

Whole cell lysates for Western blotting were extracted with PierceTM RIPA Buffer (Thermo Scientific, Rockford, IL, USA) containing protease inhibitor cocktail (Sigma, St. Louis, MO, USA). Approximately 30 micrograms of protein samples were resolved by 10% SDS-PAGE gel (Bio-Rad, 4561033) and transferred to the nitrocellulose membranes (Bio-Rad, 1704158). The primary antibodies used were 1:500 dilution of Axin1 (Cell Signaling, 2087), 1:1000 dilution of Axin2 (ab109307, Abcam), 1:1000 dilution of β-catenin (BD Biosciences, 610154,), 1:1000 dilution of BMP2 (Abcam, ab284387), 1:1000 dilution of Runx2 (HUABIO, ET1612-47), 1:1000 dilution of GAPDH (Cell Signaling, 2118). Blots were incubated with horseradish peroxi-dase-conjugated secondary antibody and then visualized by Bio-Rad enhanced chemiluminesence system using the SuperSignalTM West Pico PULS Chemiluminescent Substrate (Thermo Scientific, 34577).

Statistical analyses

The data were analyzed statistically using GraphPad Prism and presented as the mean ± SD. Two-tailed, unpaired Student's *t*-test were used to compare two groups and one-way ANOVA followed by Tukey Post-Hoc test were used to compare multiple groups of data, separately. It is considered to have significance when $P<0.05$.

RESULTS

Deletion of *Axin1* in limb MSCs leads to defects in upper limb development

Axin1 is recognized as a member of the 'destruction complex' that negatively regulates β-catenin. However, emerging reports indicated that it may have additional functions beyond its role as a scaffold protein. To elucidate the precise functional role of Axin1 in skeletogenesis, *Axin1*$^{flox/flox}$ mice were bred with *Prrx1-Cre* transgenic mice to generate *Axin1*^{Prrx1} conditional knockout (*Axin1* cKO) mice.[24,25] The *Prrx1* promoter controls Cre expression in *Prrx1-Cre* transgenic mice with the paired-related homeobox gene 1 (*Prrx1*) regula-

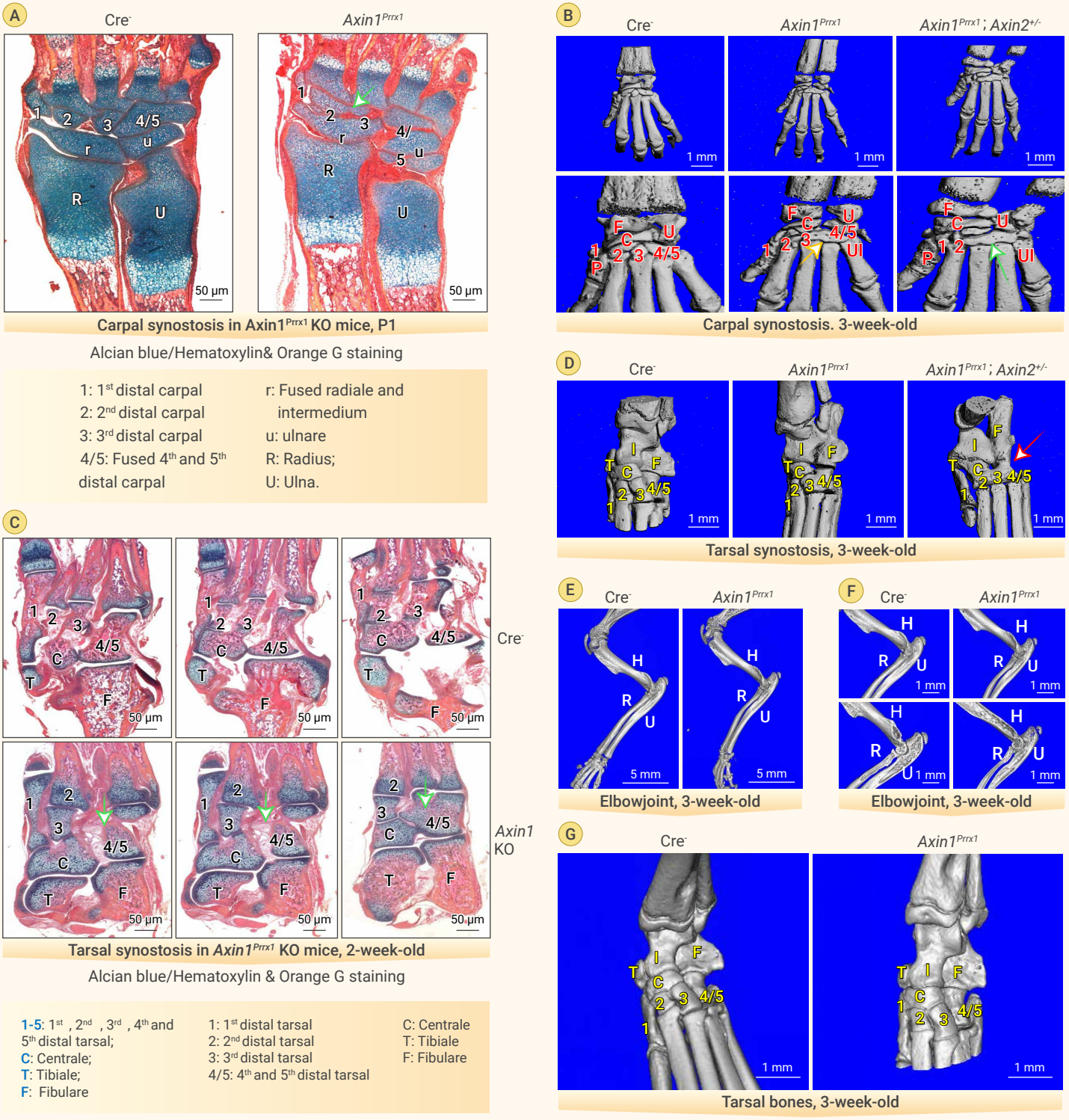

Figure 3. Fusion of carpal and tarsal bone in *Axin1* cKO mice and *Axin1*/*Axin2* dKO mice (A&B) Histological and μCT analyses showed that the 3rd distal carpal was fused with 4th/5th distal carpals (green arrow) in postnatal P1 and 3-week-old Axin1 cKO mice. In contrast, a continuous element (multiple carpal bone fused together) (green and yellow arrow) was detected in the Axin1/Axin2 dKO mice. (C&D) Results of histological (2-week-old mice) and μCT (3-week-old mice) analyses demonstrated tarsal bone fusion in Axin1 cKO mice (green arrows) and much more severe phenotype of tarsal bone fusion detected in Axin1/Axin2 dKO mice (red arrow). (E-G) Micro-CT analysis of 3-week-old Axin1 Prrx1 cKO mice showed that elbow joint and tarsal fusion phenotype could be significantly reversed when Axin2 agonist IWR-1-endo was administered into pregnant mothers at E9.5 stage.

tory element governing "Cre" expression. This leads to the removal of the floxed DNA fragment in early limb mesenchymal progenitor cells and in the population of craniofacial mesenchymal progenitor cells. One obvious defect first observed in *Axin1* cKO mice was the synovial joint fusion, particularly evident at the elbow, where the humeroradial and humeroulnar fusions were observed (Figures 1A-C). Alizarin red/Alcian blue stained skeletal preparations of forelimbs revealed joint fusion between the humerus and radius, as well as between the humerus and ulna in Axin1 cKO embryos at E13.5 and E16.5 and postnatal P7 mice (Figure 1A, red arrows). Histological examination of *Axin1* cKO forelimb sections at E16.5, P4 and P15 confirmed humeroradial fusions (Figures 1B-C). X-ray radiographic data illustrated elbow joint fusion in postnatal P12 *Axin1* cKO mice (Figure 1D). In addition,

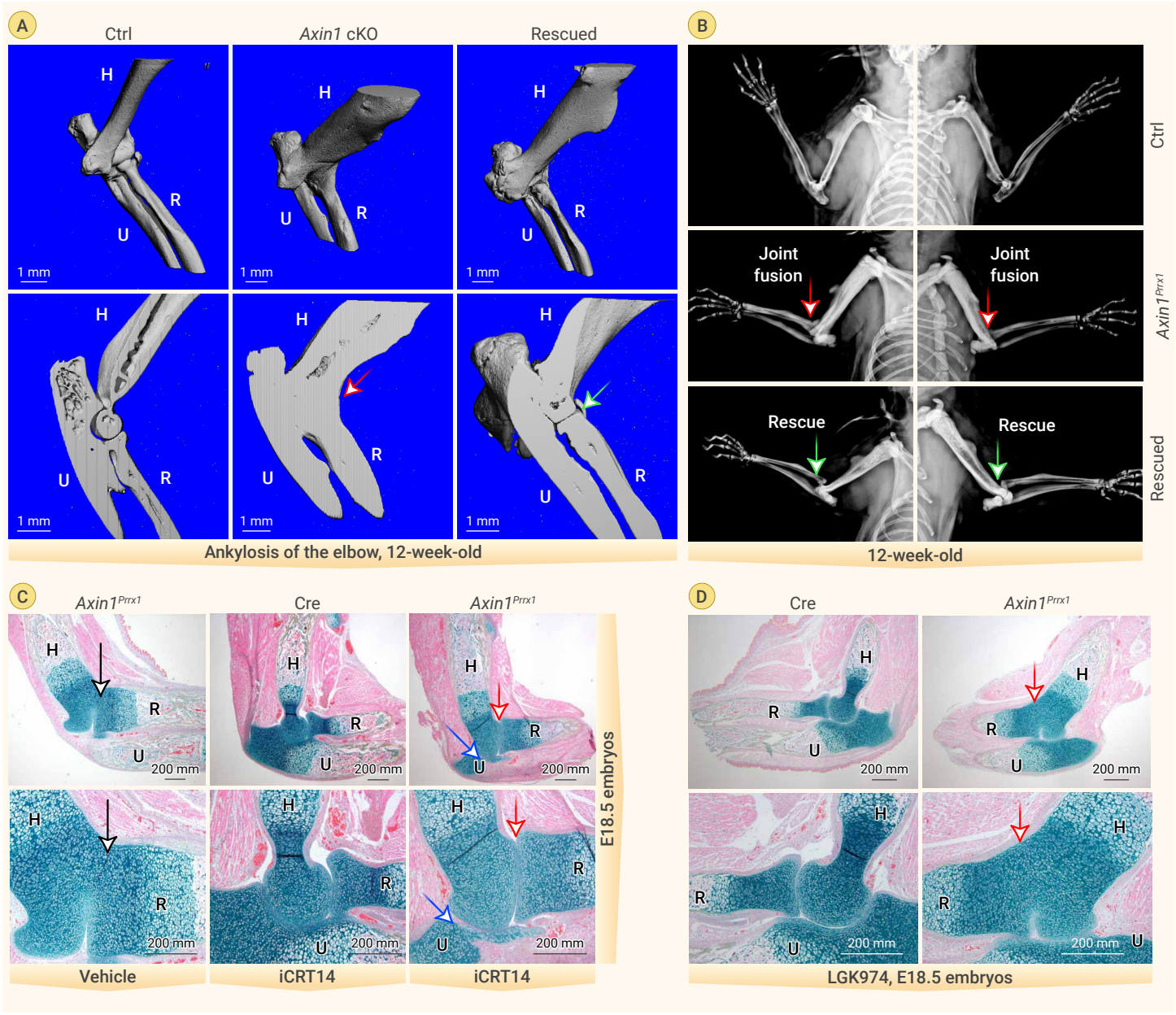

Figure 4. Inhibition of β-catenin signaling rescued upper joint defects in *Axin1* cKO mice (A) The results of μCT analysis demonstrated forelimb of 12-week-old control:(Axin1$^{flox/+}$; β-catenin$^{flox/+}$) ^{Prrx1}, Axin1 cKO: Axin1^{Prrx1}, and Rescued: (Axin1$^{flox/flox}$; β-catenin$^{flox/+}$) ^{Prrx1} mice showed that the elbow joint fusion was partially rescued in the (Axin1$^{flox/flox}$; β-catenin$^{flox/+}$) ^{Prrx1} mice group. Red arrow indicated that humerus (H) and radius (R) were fused in Axin1 cKO mice without β-catenin inhibition and that they were clearly separated in rescued mice (with β-catenin inhibition). (B) X-ray radiographic analysis of forelimb of 12-week-old mice (Axin1$^{flox/+}$; β-catenin$^{flox/+}$) ^{Prrx1} (control group), Axin1 cKO and (Axin1$^{flox/flox}$; β-catenin$^{flox/+}$) ^{Prrx1} (rescued group) showed that the defects of elbow joint fusion were partially reversed in (Axin1$^{flox/flox}$; β-catenin$^{flox/+}$) ^{Prrx1} mice. Red arrows indicated that the elbow joint fused in Axin1 cKO mice and green arrows indicated that elbow joint fusion phenotype was partially rescued in (Axin1$^{flox/flox}$; β-catenin$^{flox/+}$) ^{Prrx1} mice. (C) Inhibition of β-catenin signaling rescued the joint fusion phenotype of Axin1 cKO mice. 2.5 mg/kg iCRT14, β-catenin inhibitor was injected into pregnant mice at E9.5 stage (i.p. injection, single dose). Histological analysis showed that the humerus (H), radius (R), and ulna (U) were clearly separated in E18.5 Axin1 cKO embryos (red and blue arrows) which were treated with iCRT14. In contrast, the humerus (H) and radius (R) remained fused in E18.5 embryos of Axin1 cKO embryos treated with vehicle only (black arrows). Lower panels: higher magnification. (D) 2.5 mg/kg LGK974 was injected into pregnant mice at E9.5 stage (i.p. injection, single dose). The E18.5 embryos were analyzed. Histological results demonstrated that administration of LGK974 did not affect the elbow joint fusion (red arrows) in Axin1 cKO embryos.

Alizarin red/Alcian blue staining of E17.5 *Axin1*^{Prrx1} embryos showed hypoplastic alae of the nose (Figure 1E, red arrow).

Axin1/*Axin2* double mutant mice have severe defects in upper limb development

The Axin family comprises two members, Axin1 and Axin2, with Axin2 being the homologue of Axin1 and sharing 44% identical amino acid sequence.[26,29] The mechanisms underlying the regulation of joint formation by Axin2 remains inconclusive. Previous studies demonstrated that *Axin2* null mice (*Axin2*$^{-/-}$) presented with craniofacial defects,[13] and we previously identified a high bone mass phenotype in adult *Axin2*$^{-/-}$ mice.[14] In this study, we hypothesized that the deletion of *Axin2* in conjunction with *Axin1* could result in a more severe phenotype than the loss of Axin1 alone. To test this hypothesis, we then generated *Axin1*^{Prrx1};*Axin2*$^{+/-}$ dKO mice. Immunohistochemical analysis revealed a significant reduction in Axin1 expression in *Axin1*^{Prrx1} cKO mice, and a reduction in both Axin1 and Axin2 in *Axin1*/*Axin2* dKO mice (Figures S1A-D). By removing the negative regulators of β-catenin signaling, both *Axin1* cKO and *Axin1*/*Axin2* dKO mice exhibited upregulated β-catenin protein levels (Figures S2A-B), verifying inhibition of β-catenin degradation upon deletion of *Axin1* or *Axin1*/*Axin2* genes. Radiographic analysis (x-ray) illustrated that the size of 3-week-old *Axin1*/*Axin2* dKO mouse was smaller than that of Cre-negative controls (Figure 2A). Three-dimensional volumetric reconstructions of craniofacial bones revealed a high bone mass phenotype (Figure 2B). Observations of 3D and 2D μCT images of elbow joint clearly

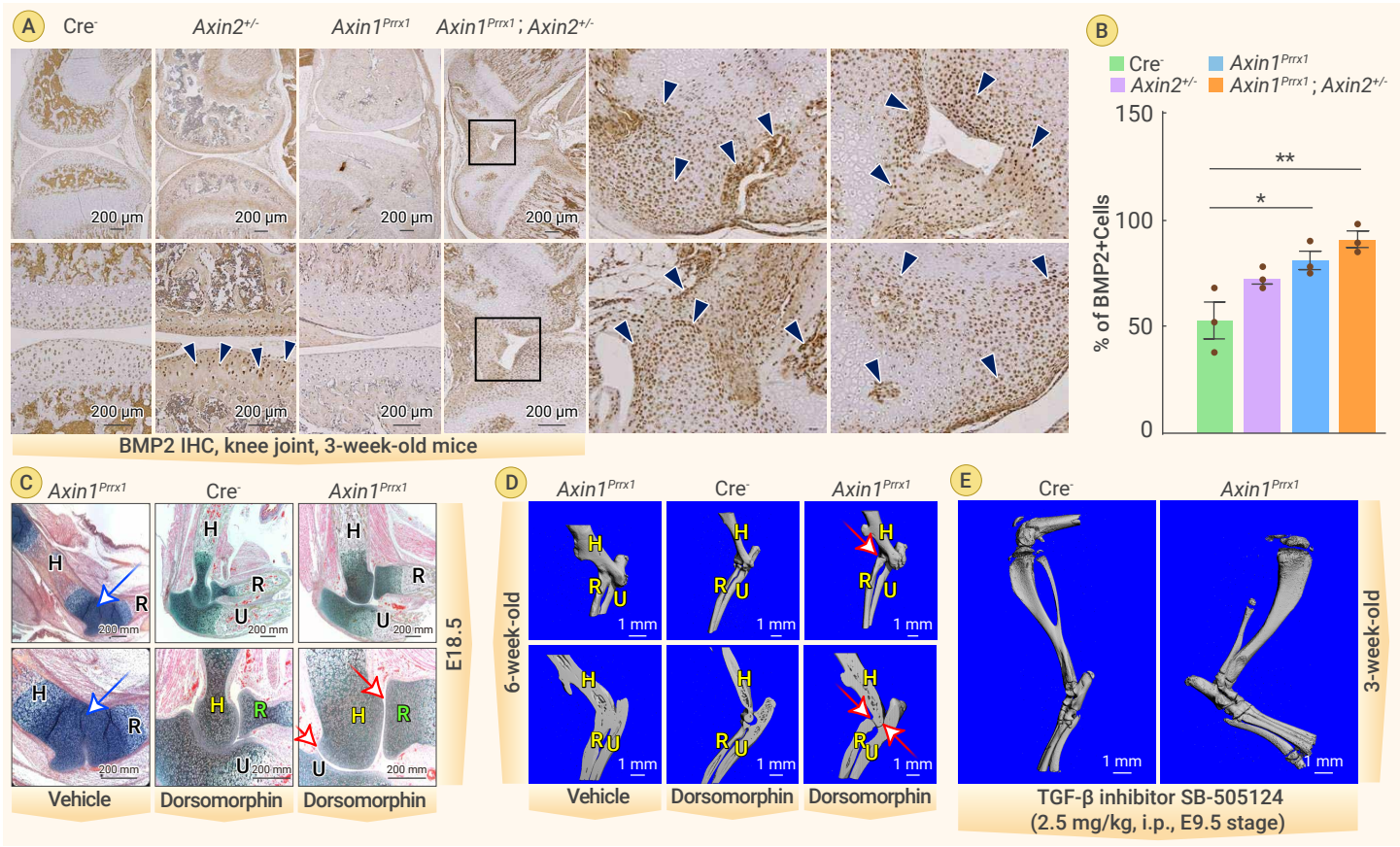

Figure 5. Inhibition of BMP signaling rescued upper joint defects in *Axin1* cKO mice (A&B) Immunohistochemical (IHC) analysis was performed to examine changes in BMP2 expression after Axin1 deletion. The results of IHC staining and quantification of BMP2 expression demonstrated that BMP2 expression was upregulated in Axin$^{2+/-}$ KO mice and Axin1/Axin2 dKO mice. Data were analyzed by one-way ANOVA followed by the Tukey Post-Hoc test. (C) Inhibition of β-catenin signaling rescued the joint fusion phenotype of Axin1 cKO mice. β-catenin inhibitor, iCRT14, was injected into pregnant mice at E9.5 stage (2.5 mg/kg, i.p. injection, single dose). Histological analysis showed that the humerus (H), radius (R), and ulna (U) were clearly separated in E18.5 Axin1 cKO embryos (red arrows) which were treated with iCRT14. In contrast, the humerus (H) and radius (R) remained fused in E18.5 embryos of Axin1 cKO embryos treated with vehicle only (blue arrows). Lower panels: higher magnification. (D) μCT analysis showed that in the elbow joint the humerus (H), radius (R) and ulna (U) were clearly separated (red arrows) after the treatment with dorsomorphin (BMP inhibitor) in 6-week-old mice. (E) In contrast, no significant changes were observed when same concentration of TGF-β inhibitor (SB-505124) was given to the pregnant mice at E9.5 stage.

demonstrated the fusion of humerus (H) and radius (R) (Figure 2C, red arrows) and the fusion of humerus and ulna (U) (Figure 2C, yellow arrows) in 4-week-old *Axin1* cKO mice. Similar fusions were also observed in 3-week-old *Axin1* cKO mice and *Axin1*/*Axin2* dKO mice (Figure 2D, green and yellow arrows). In addition to the fusion in elbow joint, defects in deltoid tuberosity development were noted in 3- and 6-week-old *Axin1* cKO mice (Figures 2E-F), with *Axin1*/*Axin2* dKO mice showing even more severe defects, including the complete loss of deltoid tuberosity (Figures 2E-F). Joint synostoses phenotype was also examined in the knee joint in *Axin1*/*Axin2* dKO mice, and histology analysis revealed the defects in the knee joint, exhibited as hypoplastic development and joint fusion at 3 weeks of age (Figure 2G).

Axin1/*Axin2* double mutant mice have severe carpal and tarsal synostoses phenotype

In addition to the joint fusion, both the *Axin1* cKO mice and *Axin1*/*Axin2* dKO mice exhibit carpal and tarsal synostoses phenotypes. Histology analysis revealed the fusion of the 3rd distal carpal element with the 4th/5th distal carpal elements in *Axin1* cKO mice (postnatal P1) (Figure 3A). The wrist joint of the *Axin1*/*Axin2* dKO mice showed a more severe phenotype, with the 3rd , 4th/5th distal carpals, ulnare (U), and ulnar sesamoid (Ul) forming a continuous element in 3-week-old *Axin1*/*Axin2* dKO mice (Figure 3B). Consistent with the observed joint fusion phenotype in the forepaw, the hindpaw synostoses were also noted in *Axin1* cKO mice and *Axin1*/*Axin2* dKO mice. Histology analysis demonstrated the fusion of the 3rd tarsal element with the 4th/5th tarsal elements in 2-week-old *Axin1* cKO mice (Figure 3C), while the centrale, 2nd, 3rd, and 4th/5th tarsal elements were fused into a continuous bony structure in *Axin1*/*Axin2* dKO mice (Figure 3D). Previous studies had associated the fusion of the 3rd and 4th/5th tarsal bones with the fibular hemimelia phenotype.[23] In this study, *Axin1*/*Axin2* dKO mice exhibited a much more severe tarsal synostosis phenotype. These findings emphasize the essential roles of both Axin1 and Axin2 in synovial joint development, indicating that endogenous Axin2 can partially compensate for the loss of Axin1 during joint formation. To assess the significance of Axin1 and Axin2 cross-reaction, pregnant *Axin1* cKO mice were administrated the Axin2 agonist IWR-1-endo at the E9.5 stage. The results demonstrate that the administration of Axin2 agonist significantly rescued the joint fusion phenotype in elbow and tarsal joints in *Axin1* cKO mice (Figure 3E).

Axin1 collaborates with GSK-3β to induce β-catenin degradation and negatively regulate β-catenin function,[30,31] and the deletion of *Axin1* leads to an increase in the expression level of β-catenin protein. We hypothesize that the skeletal defects observed in *Axin1* cKO mice result from a transient upregulation of β-catenin signaling, and reducing the *β-catenin* gene dosage can partially or completely redeem joint fusion defects in *Axin1* cKO mice. To test the hypothesis, we analyzed the interactions between *Axin1* and *β-catenin* in Cre-negative control mice, *Axin1* cKO, mice, and *Axin1*/*β-catenin* double mutant mice (*Axin1*$^{flox/flox}$;*β-catenin*$^{flox/+}$;*Prrx1-Cre*) at specific developmental stage. We observed that defects in elbow joint in *Axin1*^{Prrx1} cKO mice were partially alleviated in *Axin1*/*β-catenin* double mutant mice (Figures 4A-B). The humerus and radius and humerus and ulna (green arrows) were clearly separated in *Axin1*/*β-catenin* double mutant mice, although the joint is still dislocated (Figure 4B). To further elucidate the role of β-catenin in upper limb development, pregnant *Axin1*^{Prrx1} mice at the E9.5 stage were treated with a single dose of 2.5 mg/kg iCRT14 (β-catenin inhibitor, i.p. injection). It is known that iCRT14 disrupts the interaction between β-catenin and TCF4 and specifically inhibits β-catenin-induced gene transcription.[32] Analysis of embryos at the E18.5 stage revealed that the fusion of the elbow joint in

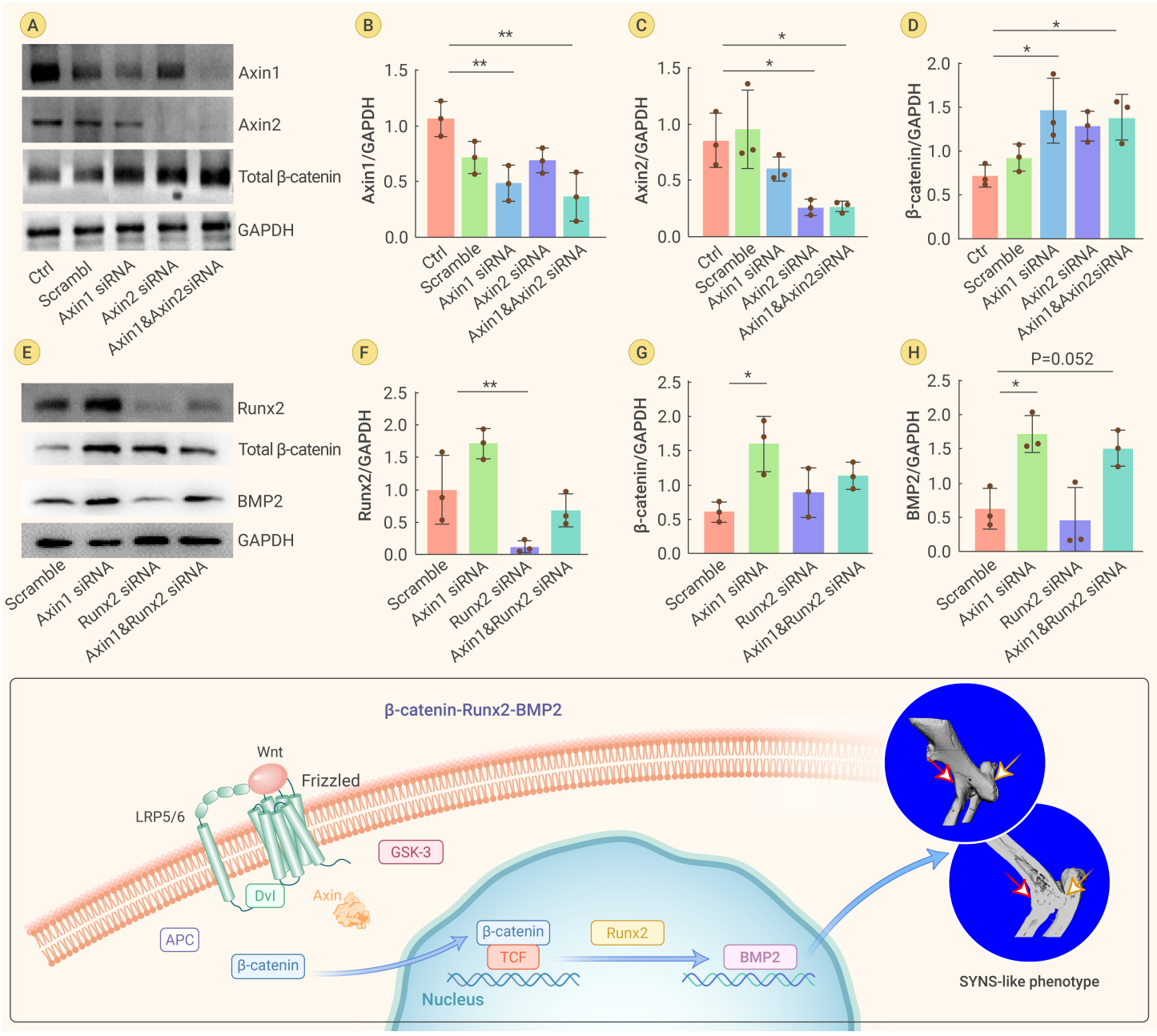

Figure 6. Upregulation of BMP2 induced by inhibition of Axin1 (or Axin1/Axin2) was mediated by Runx2 (A) Axin1 and Axin2 siRNAs were transfected into C3H10T/1/2 cells and Western blot was performed to examine expressions of Axin1, Axin2 and β-catenin. The results showed that transfection of Axin1 or bothe Axin1 and Axin2 could significantly upregulate β-catenin protein levels. (B) Transfection of Axin1 siRNA upregulated Runx2 and BMP2 expression. Co-transfection of Axin1 and Runx2 siRNA could inhibit BMP2 expression induced by Axin1 siRNA, suggesting Axin1 siRNA-induced BMP2 expression was mediated by Runx2. (C) The diagram showing that β-catenin-BMP2 signaling activation caused by inhibition of Axin1 could lead to SYNS-like phenotype in mice.

Axin1 cKO mice was significantly reversed with iCRT14 treatment (Figure 4C). These results further support the notion that β-catenin activation is a major signaling event when *Axin1* gene is deleted. In contrast, LGK974, the small molecular weight inhibitor of Wnt secretion,[33] did not reverse the joint fusion defects in *Axin1* cKO mice (Figure 4D). These results indicate that Axin1 specifically regulates joint formation through the β-catenin pathway.

It has been documented that BMP signaling plays a crucial role in synovial joint formation,[34] and the *Axin1* cKO mice exhibit multiple joint fusions that resemble the phenotype observed in *noggin* mutant mice.[35] On the other hand, it is plausible that the BMP signaling pathway is one of those immediate downstream pathways of Axin1/β-catenin signaling during skeletal development. Previous studies had indicated the upregulation of Bmp2 and Bmp4-expression in *Axin2* KO mice.[13,14] In this study, we verified and quantified BMP2 expression in joint tissues of *Axin1* cKO mice and *Axin1*/*Axin2* dKO mice. IHC results revealed a significant upregulation of BMP2 expression in the articular cartilage of *Axin2*$^{+/-}$ KO mice and in the articular cartilage, meniscus, and subchondral bone area of the knee joint in *Axin1*/*Axin2* dKO mice (Figures 5A-B). To further explore this possibility, pregnant *Axin1* cKO mice at E9.5 stage were intraperitoneally administered to dorsomorphin (a BMP signaling inhibitor),[36] or vehicle. Subsequent analysis of E18.5 embryos showed that Alcian blue/H&E staining on elbow joint sections revealed clear separation of the humerus (H), radius (R), and ulna (U) in *Axin1* cKO embryos treated with BMP inhibitor (Figure 5C). μCT scanning confirmed a significant rescue of the elbow joint fusions phenotype in 6-week-old *Axin1* cKO mice through dorsomorphin administration (Figure 5D). In contrast, dorsomorphin had no effect on joint formation in the control group mice (Figure 5D). It is worth noting that inhibition of TGF-β signaling with the small chemical inhibitor SB-505124 at the same concentration did not reverse the joint fusion defects presented in *Axin1* cKO mice (Figure 5E). Taken together, these results suggest that BMP signaling is an important downstream target of the

Axin1/β-catenin signaling pathway during limb development.

Molecular mechanisms of Axin-β-catenin-BMP2 signaling

To investigate whether Axins deficiency alters the expression of the upstream of Wnt/β-catenin signaling pathway, we examined the expression of *Wnt3a*, *Lrp5*, and *Lrp6*. The RNA expression levels of *Wnt3a, Lrp5,* and *Lrp6* showed no obvious differences in cells when *Axin1* and *Aixn2* were knocked down (Figure S3). IHC results also demonstrated that no significant changes in LRP5 and LRP6 proteins were detected in *Axin1*^{Prrx1} cKO mice compared to Cre negative control mice (Figure S3).

To further elucidate the mechanisms by which Axin1/Axin2 regulate BMP2 expression, we employed an *in vitro* siRNA knockdown approach using C3H10T1/2 mesenchymal cells. We first determined the knockdown efficiency of *Axin1* and *Axin2* siRNA in C3H10T1/2 cells and found that *Axin1* and *Axin2* expression was significantly decreased after siRNA transfection (Figures 6A-D). The expression of *Col10a1* (Figure S4E) was upregulated, while the expression of *β-catenin* and *Col2* showed no significant changes after *Axin1* and *Axin2* genes were knocked-down (Figures S4C-D). Western blot analysis demonstrated a significant reduction in Axin1 and Axin2 expression and an upregulation of β-catenin and BMP2 expression in cells with *Axin1* and *Axin2* deficiency (Figures 6E-H). When Runx2 mRNA was downregulated by Runx2 siRNA, the upregulated BMP2 expression due to *Axin1*/*Axin2* knockdown was significantly decreased, indicating that Axin-regulated BMP2 expression is mediated by Runx2 (Figures 6E-H).

DISCUSSION

SYNS is a disease characterized by the progressive fusion of multiple joints, and individuals with this disease often experience conductive hearing loss. Mutations in several genes encoding proteins critical for BMP and FGF signaling, including NOG, GDF5, GDF6, and FGF9,[5-12] have been found to be responsible for SYNS. To date, three FGF9 variants have been identified to be involved in SYNS, resulting in hand and feet joint synostoses, as well as fusion of the elbow and vertebral lumbar joints.[12] In addition, individuals with FGF9 mutations exhibit defects in craniosynostosis.[9] These genes mutations lead to disruptions in BMP and FGF signaling pathways; nonetheless, the contribution of Axin/β-catenin signaling in SYNS development has not been investigated before. It is known that BMP signaling molecules play a crucial role in skeletal development and joint formation.[7,37] Nevertheless, the contributions of Axin/β-catenin signaling in the development and progression of SYNS remain unknown.

Based on the comprehensive results presented above, the generated *Axin1* cKO mice display a phenotype characterized by fusions of the elbow joint, knee joint, carpal bones, and hypoplastic alae of the nose. These phenotypes are highly relevant to human SYNS disease as reported in clinical cases.[1,2] The establishment of the *Axin1* cKO mice and the *Axin1/Axin2* dKO mouse model in this study aims to unravel the pathogenesis of SYNS. Our findings strongly indicate that Axin1 plays a crucial role in the SYNS-like phenotype in mice and may also contribute to the human condition of SYNS. The *Axin1* cKO mice exhibit a SYNS phenotype involving humeroradial, humeroulnar, carpal, and tarsal joints. Furthermore, *Axin1*/*Axin2* dKO mice display a severe joint abnormality phenotype. Our data emphasize the fundamental role of Axin1 in synovial joint formation, with *Axin1* cKO mice exhibiting a SYNS-like phenotype. Notably, the joint fusion observed in *Axin1* cKO and *Axin1*/*Axin2* dKO mice resembles the phenotype of *noggin* mutant mice,[35] where noggin is reported as a secreted BMP antagonist. AddItionally, we demonstrate the interaction between β-catenin and BMP signaling in joint tissues during skeletal development. Consistent with our findings, previous studies with *Axin2* KO mice showed a craniosynostosis phenotype,[13] supporting the involvement of Axin family members in SYNS pathogenesis. Although previous studies have suggested the relevance between Axin1 and FGF signaling,[15] the detailed molecular mechanisms underlying the interaction between Axin1/β-catenin and FGF signaling pathways in SYNS development require further investigation.

As stated above, our observation of joint synostosis in Axin1 cKO mice closely resembles the phenotype observed in *noggin* mutant mice.[35] These findings further suggest that BMP signaling pathway could be one of the critical downstream targets of Axin1/β-catenin signaling during limb development (Figure 6E). Our study further demonstrates a significant enhancement of BMP2 protein expression in *Axin1*/*Axin2* dKO mice. More importantly, the inhibition of BMP signaling effectively reverses joint fusion defects in *Axin1* cKO mice. This implies that β-catenin may function as a central mediator, integrating BMP and/or other signaling pathways, such as FGF signaling, to regulate the SYNS development.

Our studies reveal that Axin1 exerts a significant role in coordinating the integration of β-catenin and BMP signaling pathways. Without the presence of Wnt ligands, β-catenin is phosphorylated by the 'destruction complex' containing Axin1 and Axin2. Upon the binding of Wnt ligands to the receptors or the absence of a key molecule within the destruction complex (i.e., *Axin1* KO), the phosphorylation of β-catenin is inhibited, leading to the activation of β-catenin/TCF transcriptional activation and enhancement of downstream BMP signaling ultimately.

The established *Axin1* cKO mice and *Axin1/Axin2* dKO mice present with a phenotype including fusions of the elbow joint, knee joint, carpal bones, and hypoplastic alae of the nose. The observed phenomena in the *Axin* cKO mice highlight an extremely similar relevance and indicate promising implications of this study to the clinical SYNS research. However, the limited overlap and additional phenotype between the *Axin* KO mice and clinical SYNS, such as the absence of progressive fusion of the bones of the middle ear and the additional fusions of elbow and knee need to be investigated in future studies as they are not part of the human syndrome.

In this report, we have demonstrated for the first time that the inactivation of *Axin1* or both *Axin1/Axin2* leads to SYNS-like phenotype. Significantly, this phenotype can be partially rescued by the inhibition of β-catenin or BMP signaling. These findings imply that the temporal and transient activation of β-catenin-BMP signaling is the key event in SYNS pathogenesis. This novel revelation holds promise for the development of new therapeutic strategies aimed at the effectively treating this genetic disease.

REFERENCES

1. Elkington, S.G., and Huntsman, R.G. (1967). The Talbot fingers: A study in symphalangism. Br. Med. J. **1**: 407–411. DOI: 10.1136/bmj.1.5537.407.
2. Pan, Z., Lu, W., Li, X., et al. (2020). Multiple synostoses syndrome: Clinical report and retrospective analysis. Am. J. Med. Genet. A **182**: 1438–1448. DOI: 10.1002/ajmg.a.61583.
3. Higashi, K., and Inoue, S. (1983). Conductive deafness, symphalangism, and facial abnormalities: The WL syndrome in a Japanese family. Am. J. Med. Genet. **16**: 105–109. DOI: 10.1002/ajmg.1320160116.
4. Dobson, S.M., Kiss, C., Borschneck, D., et al. (2022). Novel FGF9 variant contributes to multiple synostoses syndrome 3. Am. J. Med. Genet. A **188**: 2162–2167. DOI: 10.1002/ajmg.a.62729.
5. Lee, B.H., Kim, O.H., Yoon, H.K., et al. (2014). Variable phenotypes of multiple synostosis syndrome in patients with novel NOG mutations. Joint Bone Spine **81**: 533–536. DOI: 10.1016/j.jbspin.2014.07.006.
6. Debeer, P., Huysmans, C., Van de Ven, W.J., et al. (2005). Carpal and tarsal synostoses and transverse reduction defects of the toes in two brothers heterozygous for a double de novo NOGGIN mutation. Am. J. Med. Genet. A **134**: 318–320. DOI: 10.1002/ajmg.a.30645.
7. Dawson, K., Seeman, P., Sebald, E., et al. (2006). GDF5 is a second locus for multiple-synostosis syndrome. Am. J. Hum. Genet. **78**: 708–712. DOI: 10.1086/503204.
8. Clarke, R.A., Fang, Z., Murrell, D., et al. (2021). GDF6 knockdown in a family with multiple synostosis syndrome and speech impairment. Genes (Basel) **12**: 1354. DOI: 10.3390/genes12091354.
9. Rodriguez-Zabala, M., Aza-Carmona, M., Rivera-Pedroza, C.I., et al. (2017). FGF9 mutation causes craniosynostosis along with multiple synostoses. Hum. Mutat. **38**: 1471–1476. DOI: 10.1002/humu.23292.
10. Tang, L., Wu, X., Zhang, H., et al. (2017). A point mutation in Fgf9 impedes joint interzone formation leading to multiple synostoses syndrome. Hum. Mol. Genet. **26**: 1280–1293. DOI: 10.1093/hmg/ddx029.
11. Thuresson, A.C., Croft, B., Hailer, Y.D., et al. (2021). A novel heterozygous variant in FGF9 associated with previously unreported features of multiple synostosis syndrome 3. Clin. Genet. **99**: 325–329. DOI: 10.1111/cge.13880.
12. Sentchordi-Montane, L., Diaz-Gonzalez, F., Catedra-Valles, E.V., et al. (2021). Identification of the third FGF9 variant in a girl with multiple synostosis-comparison of the genotype: Phenotype of FGF9 variants in humans and mice. Clin. Genet. **99**(2): 309–312. DOI: 10.1111/cge.13876.
13. Yu, H.M., Jerchow, B., Sheu, T.J., et al. (2005). The role of Axin2 in calvarial morphogenesis and craniosynostosis. Development **132**: 1995–2005. DOI: 10.1242/dev.01786.
14. Yan, Y., Tang, D., Chen, M., et al. (2009). Axin2 controls bone remodeling through the

beta-catenin-BMP signaling pathway in adult mice. J. Cell Sci. **122**: 3566-3578. DOI: 10.1242/jcs.051904.
15. Zhou, Y., Shu, B., Xie, R., et al. (2019). Deletion of Axin1 in condylar chondrocytes leads to osteoarthritis-like phenotype in temporomandibular joint via activation of beta-catenin and FGF signaling. J. Cell Physiol. **234**: 1720–1729. DOI: 10.1002/jcp.27043.
16. Biechele, S., Cox, B.J., and Rossant, J. (2011). Porcupine homolog is required for canonical Wnt signaling and gastrulation in mouse embryos. Dev. Biol. **355**: 275–285. DOI: 10.1016/j.ydbio.2011.04.029.
17. Kondo, N., Yuasa, T., Shimono, K., et al. (2011). Intervertebral disc development is regulated by Wnt/beta-catenin signaling. Spine (Phila Pa 1976) **36**: E513-518. DOI: 10.1097/BRS.0b013e3181f52cb5.
18. Clevers, H., and Nusse, R. (2012). Wnt/beta-catenin signaling and disease. Cell **149**: 1192–1205. DOI: 10.1016/j.cell.2012.05.012.
19. Xie, L., Wang, G., Wu, Y., et al. (2021). Programmed surface on poly(aryl-ether-ether-ketone) initiating immune mediation and fulfilling bone regeneration sequentially. The Innovation **2**: 100148. DOI: 10.1016/j.xinn.2021.100148.
20. Xu, Y., Li, Y., Gao, A., et al. (2023). Gasotransmitter delivery for bone diseases and regeneration. The Innovation Life **1**: 100015. DOI: 10.59717/j.xinn-life.2023.100015.
21. Baron, R., and Kneissel, M. (2013). WNT signaling in bone homeostasis and disease: from human mutations to treatments. Nat. Med. **19**: 179–192. DOI: 10.1038/nm.3074.
22. Regard, J.B., Zhong, Z., Williams, B.O., et al. (2012). Wnt signaling in bone development and disease: Making stronger bone with Wnts. Cold Spring Harb. Perspect. Biol. **4**. DOI: 10.1101/cshperspect.a007997.
23. Xie, R., Yi, D., Zeng, D., et al. (2022). Specific deletion of Axin1 leads to activation of beta-catenin/BMP signaling resulting in fibular hemimelia phenotype in mice. Elife **11**: e80013. DOI: 10.7554/eLife.80013.
24. Xie, R., Jiang, R., and Chen, D. (2011). Generation of Axin1 conditional mutant mice. Genesis **49**: 98–102. DOI: 10.1002/dvg.20703.
25. Zeng, L., Fagotto, F., Zhang, T., et al. (1997). The mouse Fused locus encodes Axin, an inhibitor of the Wnt signaling pathway that regulates embryonic axis formation. Cell **90**: 181–192. DOI: 10.1016/s0092-8674(00)80324-4.
26. Logan, M., Martin, J.F., Nagy, A., et al. (2002). Expression of Cre Recombinase in the developing mouse limb bud driven by a Prxl enhancer. Genesis **33**: 77–80. DOI: 10.1002/gene.10092.
27. Brault, V., Moore, R., Kutsch, S., et al. (2001). Inactivation of the beta-catenin gene by Wnt1-Cre-mediated deletion results in dramatic brain malformation and failure of craniofacial development. Development **128**: 1253–1264. DOI: 10.1242/dev.128.8.1253.
28. McLeod, M.J. (1980). Differential staining of cartilage and bone in whole mouse fetuses by alcian blue and alizarin red S. Teratology **22**: 299–301. DOI: 10.1002/tera.1420220306.
29. Behrens, J., Jerchow, B.A., Wurtele, M., et al. (1998). Functional interaction of an axin homolog, conductin, with beta-catenin, APC, and GSK3beta. Science **280**: 596–599. DOI: 10.1126/science.280.5363.596.
30. Li, V.S., Ng, S.S., Boersema, P.J., et al. (2012). Wnt signaling through inhibition of beta-catenin degradation in an intact Axin1 complex. Cell **149**: 1245–1256. DOI: 10.1016/j.cell.2012.05.002.
31. Kim, S.E., Huang, H., Zhao, M., et al. (2013). Wnt stabilization of beta-catenin reveals principles for morphogen receptor-scaffold assemblies. Science **340**: 867–870. DOI: 10.1126/science.1232389.
32. Gonsalves, F.C., Klein, K., Carson, B.B., et al. (2011). An RNAi-based chemical genetic screen identifies three small-molecule inhibitors of the Wnt/wingless signaling pathway. Proc. Natl. Acad. Sci. U. S. A. **108**: 5954–5963. DOI: 10.1073/pnas.1017496108.
33. Liu, J., Pan, S., Hsieh, M.H., et al. (2013). Targeting Wnt-driven cancer through the inhibition of Porcupine by LGK974. Proc. Natl. Acad. Sci. U. S. A. **110**: 20224–20229. DOI: 10.1073/pnas.1314239110.
34. Gong, Y., Krakow, D., Marcelino, J., et al. (1999). Heterozygous mutations in the gene encoding noggin affect human joint morphogenesis. Nat. Genet. **21**: 302–304. DOI: 10.1038/6821.
35. Brunet, L.J., McMahon, J.A., McMahon, A.P., et al. (1998). Noggin, cartilage morphogenesis, and joint formation in the mammalian skeleton. Science **280**: 1455–1457. DOI: 10.1126/science.280.5368.1455.
36. Yu, P.B., Hong, C.C., Sachidanandan, C., et al. (2008). Dorsomorphin inhibits BMP signals required for embryogenesis and iron metabolism. Nat. Chem. Biol. **4**: 33–41. DOI: 10.1038/nchembio.2007.54.
37. Bandyopadhyay, A., Tsuji, K., Cox, K., et al. (2006). Genetic analysis of the roles of BMP2, BMP4, and BMP7 in limb patterning and skeletogenesis. PLoS Genet. **2**: e216. DOI: 10.1371/journal.pgen.0020216.

FUNDING AND ACKNOWLEDGMENTS

This work was financial supported by the National Key Research and Development Program of China (2022YFA1207500), National Natural Science Foundation of China (NSFC) grants (82030067, 82161160342, 82250710174 and 82172397) We also acknowledge the Youth Innovation Promotion Association of Chinese Academy of Sciences (No. 2020353) and the GuangDong Basic and Applied Basic Research Foundation grant 2021A1515111075. The funders had no role in study design, data collection and analysis, decision to publish or preparation of the manuscript.

AUTHOR CONTRIBUTIONS

Di Chen conceived the idea, designed the experiment and supervised the research. Di Chen and Liping Tong wrote the manuscript with input from all authors. Dan Yi, Rong Xie, and Daofu Zeng carried out the experiment, collected and analyzed the data. Jun Xiao, Guozhi Xiao, and Hongting Jin provided input for data analysis and manuscript revision. All authors read and commented on the manuscript.

DECLARATION OF INTERESTS

The authors declare no competing interests.

ETHICAL STATEMENT AND PATIENT CONSENT

All mice were kept in SPF laboratory under standard conditions. Animal experiments were approved by the Animal Committee of Rush University (IACUC-14-071) and SIAT (SIAT-IACUC-240321-YYS-YD-A2518).

DATA AND CODE AVAILABILITY

All data needed to evaluate the conclusions in the paper are present in the paper. Additional data related to this paper may be requested from the authors.

SUPPLEMENTAL INFORMATION

It can be found online at https://doi.org/10.59717/j.xinn-med.2024.100053

LEAD CONTACT WEBSITE

Di Chen: https://people.ucas.ac.cn/~dichen?language=cn